


RESEARCH

Open Access



Oral colon-targeted pH-responsive polymeric nanoparticles loading naringin for enhanced ulcerative colitis therapy

Shilong Fan^{1,2}, Yue Zhao^{1,2}, Yinlian Yao^{1,2}, Xin Shen^{1,2}, Xingxing Chai³, Jiahui Li^{1,2}, Jiang Pi³, Xueqin Huang³, Hua Jin^{1,2*} and Zhikun Zhou^{1,2*} 

Abstract

An oral colon-targeted drug delivery system holds great potential in preventing systemic toxicity and preserving the therapeutic benefits of ulcerative colitis (UC) treatment. In this study, we developed a negatively charged PLGA-PEG nanoparticle system for encapsulating naringin (Nar). Additionally, chitosan and mannose were coated on the surface of these nanoparticles to enhance their mucosal adsorption and macrophage targeting abilities. The resulting nanoparticles, termed MC@Nar-NPs, exhibited excellent resistance against decomposition in the strong acidic gastrointestinal environment and specifically accumulated at inflammatory sites. Upon payload release, MC@Nar-NPs demonstrated remarkable efficacy in alleviating colon inflammation as evidenced by reduced levels of pro-inflammatory cytokines in both blood and colon tissues, as well as the scavenging of reactive oxygen species (ROS) in the colon. This oral nanoparticle delivery system represents a novel approach to treating UC by utilizing Chinese herbal ingredient-based oral delivery and provides a theoretical foundation for local and precise intervention in specific UC treatment.

Keywords Oral delivery, Colon-targeted nanoparticles, Naringin, Ulcerative colitis, Pro-inflammatory cytokines, Reactive oxygen species

Introduction

Inflammatory bowel disease (IBD) is a non-specific, inflammatory gastrointestinal disease of unknown etiology, including ulcerative colitis (UC) and Crohn's disease (CD), is a chronic inflammatory disease that occurs in the gastrointestinal tract. It is clinically characterized by severe diarrhea, abdominal pain, and bloody stools. The disease has a relapsing course, long duration, and severely affects the quality of life of patients [1]. Currently, there is no definitive cure for UC, and it has been listed as one of the modern incurable diseases by the World Health Organization. Studies have shown that patients with ulcerative colitis have a significantly higher risk of developing colorectal cancer compared to the general population [2]. Therefore, the development of safe

*Correspondence:

Hua Jin
jinhua0413@gdmu.edu.cn
Zhikun Zhou
zhouzhkun@126.com

¹Guangdong Provincial Key laboratory of research and development of Natural drugs, School of Pharmacology, Guangdong Medical University, Dongguan 523808, China

²Research Center of Nano Technology and Application Engineering, Dongguan Innovation Institute, Guangdong Medical University, Dongguan 523808, China

³Laboratory Animal Center, School of Medical Technology, Guangdong Medical University, Dongguan 523808, China



© The Author(s) 2024. **Open Access** This article is licensed under a Creative Commons Attribution-NonCommercial-NoDerivatives 4.0 International License, which permits any non-commercial use, sharing, distribution and reproduction in any medium or format, as long as you give appropriate credit to the original author(s) and the source, provide a link to the Creative Commons licence, and indicate if you modified the licensed material. You do not have permission under this licence to share adapted material derived from this article or parts of it. The images or other third party material in this article are included in the article's Creative Commons licence, unless indicated otherwise in a credit line to the material. If material is not included in the article's Creative Commons licence and your intended use is not permitted by statutory regulation or exceeds the permitted use, you will need to obtain permission directly from the copyright holder. To view a copy of this licence, visit <http://creativecommons.org/licenses/by-nc-nd/4.0/>.

and effective new drugs and treatment strategies is of great significance in alleviating and controlling the progression of UC.

Currently, anti-inflammatory drugs such as salicylates [3] and corticosteroids [4] are the main treatment options used in clinical practice for IBD. Although they have achieved certain therapeutic effects [5], their side effects is very serious, such as salicylic acid can cause nausea, headache, and severe allergic reactions, while corticosteroids can affect bone density and increase the risk of fractures, along with a higher risk of infections and other liver and kidney damages. Therefore, it is of great significance and an urgent clinical need to thoroughly explore more natural and less side-effect-supplementing and alternative drugs, as well as develop new localized targeted treatment techniques and methods [6]. These approaches can help control medication during the treatment of UC patients, reduce drug resistance and medication-related side effects, and improve the efficacy and quality of life for patients. Therefore, the search for natural drugs with lower toxicity, and the precise delivery of these drugs to the site of colonic inflammation, while not compromising their anti-inflammatory efficacy and reducing their systemic toxic side effects, represents a significant breakthrough in the clinical alleviation and effective treatment of UC.

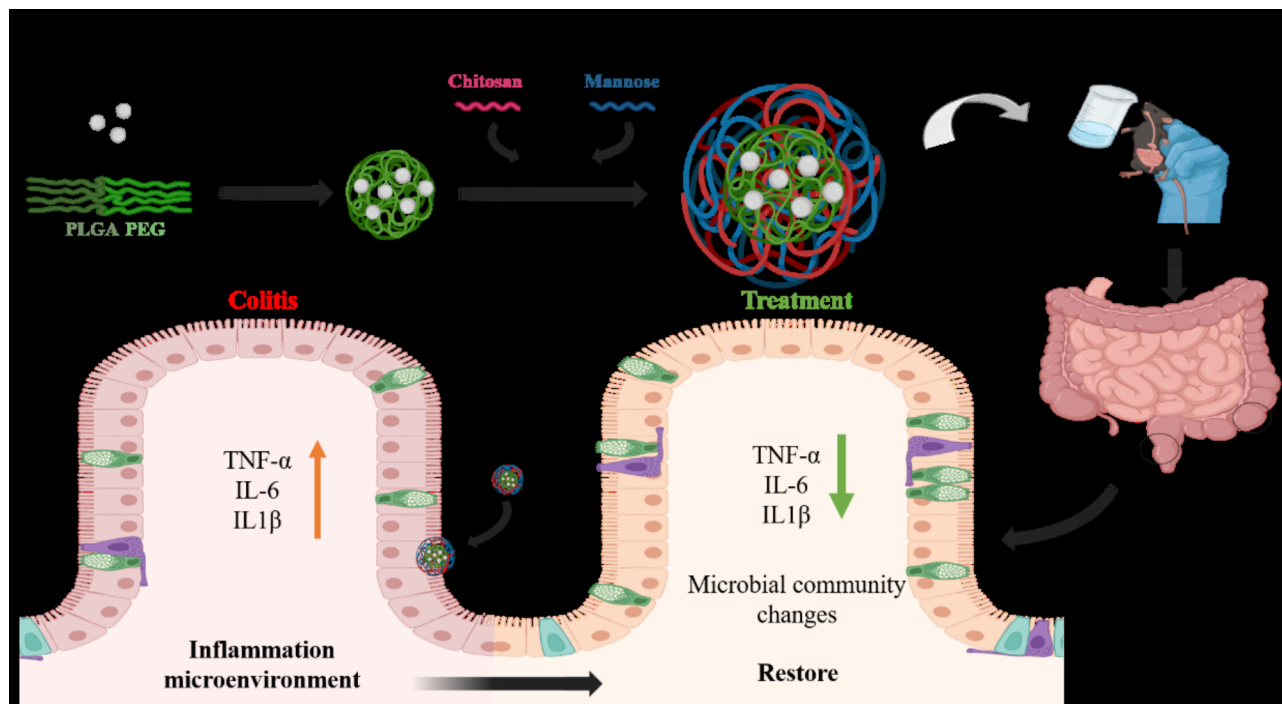
Naringin (Nar) is a natural flavonoid compound with multiple bioactivities, extracted from the dried peels of immature or nearly mature fruits of citrus plants in the Rutaceae family, such as pomelo and grapefruit. It has been confirmed to have a wide range of pharmacological activities, including anti-inflammatory, antioxidant, antiviral, antimicrobial, anticancer, anticoagulant, anti-liver fibrosis, and anti-atherosclerosis effects [7, 8]. Research has found that Nar can regulate the M2 polarization of mouse peritoneal macrophages through PPAR γ /miR-21 modulation [9]. Nar inhibits the activation of the NLRP3(Nucleotide-binding oligomerization domain, leucine-rich repeat and pyrin domain-containing 3) inflammasome and promotes M2 macrophage polarization by stimulating TFEB nuclear translocation, thereby preventing myocardial ischemia-reperfusion injury [10]. In recent years, it has been discovered in experimental colitis models that a higher dose of Nar (100 mg/kg) administered continuously for over 7 days can significantly alleviate symptoms of UC in mice [11]. Additionally, Nar can inhibit the activation of the MAPK and NLRP3 inflammasome induced by DSS, and naringin maintains the integrity of tight junction (TJ) structures by regulating the expression of ZO-1, thus repairing the intestinal barrier [12]. However, Nar has extremely low water solubility, poor absorption in conventional formulations, and low oral bioavailability. Therefore, it is of great significance to modify Nar,

develop new formulations to improve its bioavailability, enhance sustained release and targeting, and expand its clinical applications.

Various routes of administration, including intravenous injection, rectal administration, and oral administration, have been used for systemic or local drug delivery in IBD therapy. Intravenous injection always bypasses the first-pass effect and hepatic-intestinal circulation, and lower patient compliance. Rectal administration can partially reduce the first pass effect of the liver, however, rectal drug formulations must be retained in the colon for an extended period, which is a big challenge for patients with diarrhea. Oral drug delivery is considered the most ideal route for IBD treatment: it offers good patient compliance, convenient self-administration, high safety and cost-effective production. Due to the harsh environmental conditions, including strong acidic gastric fluid, abundant digestive enzymes, and a diverse range of bacterial species. These conditions tend to compromise the stability of drug formulations and diminish the efficacy of loaded medications. Therefore, drug formulations should be designed to maintain stability as they pass through the upper gastrointestinal tract and selectively release the loaded medication into inflamed intestinal tissues.

Chitosan, as a natural polysaccharide material, has extensive applications in oral drug delivery systems [13]. Due to its good biocompatibility, strong degradability, low toxicity, and strong adhesion, chitosan is widely used in drug delivery systems. In oral administration, chitosan can serve as a carrier to help drugs reach the intestinal target site stably, with controlled release to prolong the drug's release time in the body, thereby enhancing the drug's bioavailability and efficacy.

In this work, an oral nano-based drug delivery system was synthesized using simple emulsification method (Scheme 1A). Firstly, PLGA-PEG nanoparticles were designed to encapsulate Nar, and then chitosan and mannose were further coated on the surface of nanoparticles to endow these nanoparticles with the mucosal adsorption and macrophage targeting abilities. The oral nanoparticle system demonstrated an excellent resist decomposition ability against the strong acidic gastrointestinal environment, and accumulated in the specific inflammatory sites through the affinity of electrostatic reaction. The oral nanoparticles exhibit significant inflammation targeting property and can accumulate and achieve controlled drug release in the inflamed colons. After oral administration, the Nar-loaded oral nanoparticle could remarkably alleviate the colon inflammatory response, which evidenced by the decreased in secretion of pro-inflammatory cytokines TNF- α and IL-6, and scavenging reactive oxygen species in macrophages of UC mouse model (Scheme 1B). The results indicate that the as-synthesized nanocarriers have excellent colon



Scheme 1 The preparation of Naringin-loaded nanoparticles (MC@Nar-NPs) and target delivery of Nar to alleviate DSS-induced colitis in mice. (A) Preparation of Nar-encapsulated PLGA-PEG NPs by emulsification- evaporation method, and conjugation of chitosan and mannose to the surface of NPs. Upon oral administrated (B), MC@Nar-NPs preferentially accumulated in inflammatory sites in the colon due to the high expression of mannose receptors on the surface of digestive tract macrophages. Subsequently, Nar internalized by macrophages alleviated colitis through inhibition pro-inflammatory cytokine storm and scavenge oxygen free radicals

targeting capabilities and can successfully deliver the drug to the site of colonic inflammation.

Materials and methods

Materials

Naringin (Nar, 98%) was bought from Shanghai Yuanye Bio-Technology Co., Ltd. (Shanghai, China). PLGA(Mw:38000)-PEG(Mw:5000) and 2',7'-dichloro-fluorescein diacetate (DCFH-DA) kits were bought from Sigma (USA). Dichloromethane was bought from Shanghai Aladdin Bio-Chem Technology Co., LTD. MTT was obtained from Beyotime Biotech Inc. (Nanjing, China). RPMI-1640 medium, DMEM medium, Phosphate Buffer Solution, fetal bovine serum (FBS), trypsin and penicillin-streptomycin were purchased from Gibco BRL (USA).

Rabbit anti-Myeloperoxidase monoclonal antibody (abs159595) was obtained from Absin (Shanghai, China). IL-1β(ab315084), IL-6(ab290735) monoclonal antibodies were purchased from Abcam, UK. NLPR3 mAb (#15101) was purchased from cell signaling technology, USA.

All chemicals were of analytical grade.

Cells

RAW264.7 cells and Caco-2 cells were provided by the Cell Library of Guangdong Provincial Key Laboratory of Medical Molecular Diagnostics, Guangdong Medical

University. The cells were cultured in DMEM (Gibco, USA) or RPMI-1640 (Gibco, USA) with 10% fetal bovine serum (Gibco) containing 100 μg/mL streptomycin and 100 IU mL⁻¹ penicillin at 5% CO₂ and 37 °C.

Preparation of Nar-loaded nanoparticles (MC@Nar-NPs)

The MC@Nar-NPs were synthesized using emulsification and evaporation method as previously described [14] with some modifications. Briefly, 60 mg Nar and 200 mg PLGA(Mw:38000)-PEG(Mw:5000) were dissolved in 5 mL of dichloromethane as the oil phase, and this phase was homogenized for 3 min on ice. Then, 15 mL of water phase (1.5% of PVA solution, including 0.3% of chitosan/mannose and 0.5% glacial acetic acid) was added into the oil phase and followed by homogenized for 3 min on ice to form the Nar-loaded PLGA(Mw:38000)-PEG(Mw:5000) emulsification. Finally, the nanoparticles were harvested by centrifuging at 12,000 rpm for 20 min and washed 3 times using ultrapure water. The harvested nanoparticles were lyophilized for 48 h using lyophilizer for storage in powdered form.

To determine the biodistribution of NPs in cells or organs, NPs containing a fluorescent dye indocyanine green (ICG) or Coumarin 6 (C6) were prepared using the above procedure, except that 100 μg fluorescent dye was added into the oil phase. The incorporated dye acts as a

fluorescent marker for NPs and offers a sensitive method to determine qualitatively and quantitatively organs distribution or intracellular uptake using IVIS imaging system or fluorescent microscope.

Characterization of nanoparticles

The size distribution and zeta potential of the nanoparticles were determined using a Nano Particle Analyzer SZ-100 (Horiba Scientific, USA). Morphology of NPs were visualized by scanning electron microscopy (Philips Co, Holland). The encapsulation of Nar was detected using an ultraviolet and visible spectrophotometer (UV-2700, Shimadzu Corporation, Japan). 1 mg/mL of Nar and MC@Nar-NPs were diluted into 10-fold. The loading rate and concentrations of MC@Nar-NPs were measured by microplate reader (Infinite 200 pro, Swiss) at 283 nm.

Cellular uptake

The cells were cultured with C6-labeled NPs for 4 h, and washed twice with PBS to remove unbound nanoparticles. The cells were imaged using a Live Cell Imaging System (EVOSFL Auto, Invitrogen, USA).

Animal study

Male C57/6J mice (8–10 weeks) were purchased from SPF biotechnology company, LTD (Beijing, China). The experimental protocols were conducted according to National Institutes of Health guidelines on the use of laboratory animals. The animal care and study protocols were approved by the Institutional Animal Care and Use Committee of Guangdong Medical University (GDY2002094). All the experiments were performed in accordance with relevant guidelines and regulations of Animal Ethics Committee of Guangdong province, China.

Hemolysis assay

To determine the in vivo biosafety of the compounds, hemolysis of red blood cells treated with the designated compounds were performed according to the previous studies [15]. Erythrocytes were originated from normal healthy C57BL/6J mice through washing the anticoagulant whole blood with PBS at 3,000 rpm for 10 min. Then, a 5% red blood cell suspension (v/v, in PBS) was blended with different formulations of Nar. The erythrocyte sample lysed in water was used as positive control, and erythrocytes diluted in PBS was used as negative control group. After incubating with 100 µg/mL of compounds at 37 °C for 30 min, all the samples were centrifuged at 3,000 rpm, 4 °C, for 10 min to collect the supernatant and measure its absorbance value at 540 nm using microplate reader (TECAN, Switzerland).

In vivo biosafety assay

To determine the biosafety of Nar-loaded NPs in vivo, different formulations of Nar (Free Nar and MC@-NPs) were i.g. administrated to normal healthy mice (dosage: 200 µg/kg body weight, 5 mice/group) for one week, once per day. The pathological sections of main organs were stained with hematoxylin and eosin (H&E) to evaluate the toxic effects of Nar or MC@Nar-NPs. The levels of alanine transaminase (ALT) and aspartate transaminase (AST) of liver homogenate in each group were also determined using the assay kits (C010-2-1, Nanjing Jiancheng Bioengineering Institute, China).

DSS-induced UC mouse model

The 2.5% (w/v) of DSS (Dextran Sulfate Sodium Salt) solution was freshly prepared every other day to induce ulcerative colitis model. To study the therapeutic efficacy of MC@Nar-NPs, 20 mice were divided into 4 groups with 5 mice in each group: (1) normal healthy control (i.e., no treatment), (2) DSS+PBS solution, (3) DSS+free Nar (10 mg/kg), (4) DSS+MC@Nar-NPs (10 mg/kg of Nar equivalent). The experimental protocols were shown in the Fig. 5A. The mice were given DSS solution from 1st to 5th day, and at 6th day, the DSS was moved away and fresh water was replaced. At 8th day, the mice were sacrificed and specific tissues were collected.

Biodistribution of NPs in vivo

To determine the inflammatory colon-targeted properties of NPs, DSS-induced UC mice were received a single dose intragavage of ICG-labeled NPs. The mice were anesthetized using Isoflurane at the designated time points and imaged using in vivo imaging systems (IVIS) (Kodak Multi Mode) at 740/820 nm (for ICG). At the end point, mice were sacrificed to obtain and photographed the intestine, colon, and all the major organs (heart, liver, spleen, lung, and kidney). The fluorescence intensity was analyzed by the Living Imaging software.

Disease activity index (DAI) scores

DAI was determined by body weight loss, stool consistency, and stool bleeding recorded every day. The scores were evaluated according to the previous study [16]. Briefly, body weight loss (less than 1%: 0; 1%~10%: 1; 10%~15%: 2; 15%~20%: 3; and more than 20%: 4). Stool scoring (normal: 0–1; loose: 2~3; diarrhea: 4). Fecal blood (normal: 0–1; occult blood: 2~3; gross bleeding: 4).

Pro-inflammation assay

Elisa assay. Inflammatory cytokines in plasma, including IL-6, was assessed by ELISA kits (Jiangsu Meimian Industrial Co., Ltd).

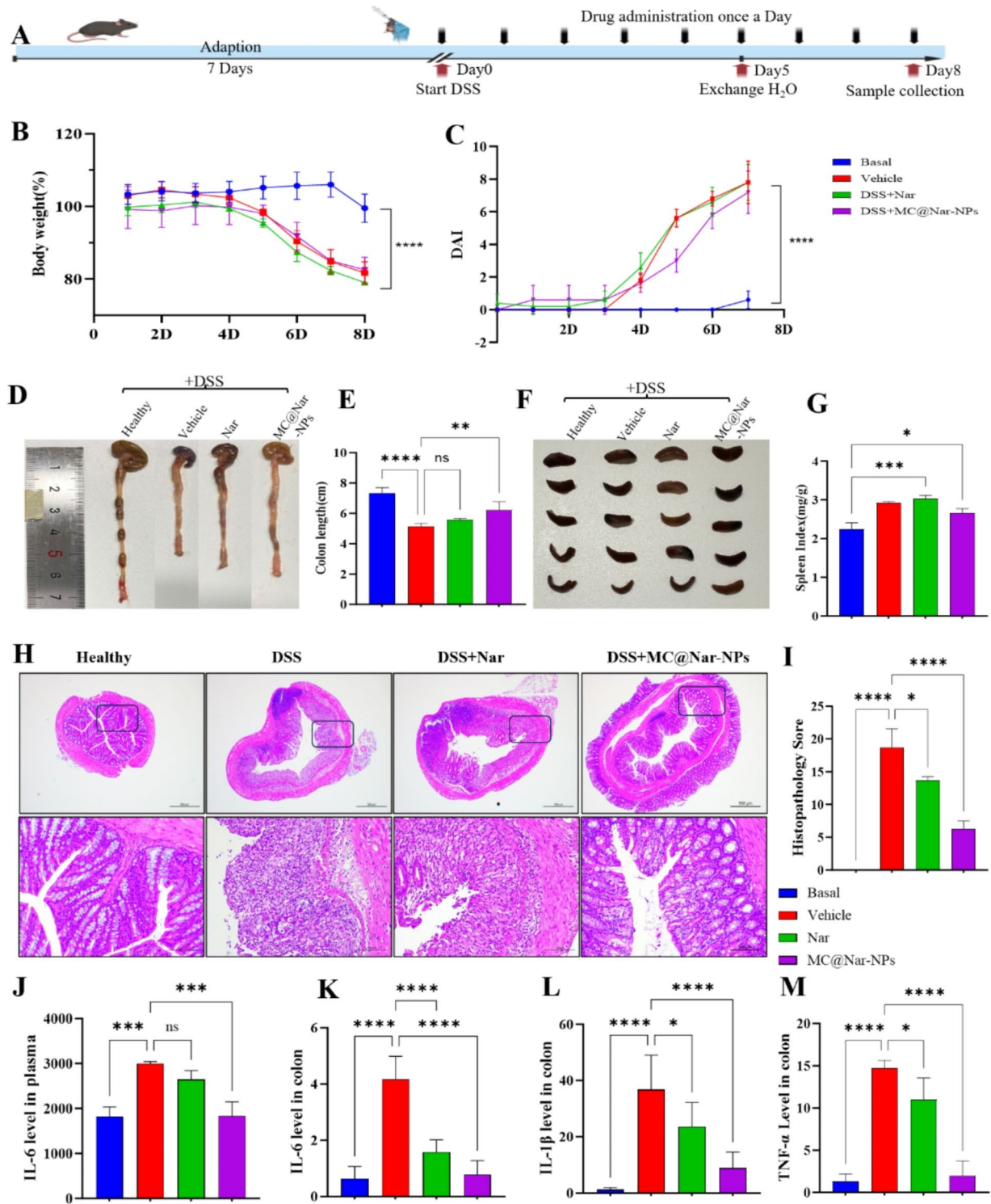


Fig. 5 Therapeutics of oral administered Nar or MC@Nar-NPs on DSS-induced UC mice. (A) Time axis of DSS-induced UC and the timing of treatment: Mice were adaptively fed for one week, then i.g. with Nar or MC@Nar-NPs at 10 mg/kg/d while drinking the 2.5% DSS water freely for 5 days, fresh water was changed from the 6th day, after 72 h of fresh water, the mice was euthanized and collected samples. (B-C) Variation of body weight and DAI scores in different treated groups during experimental process. (D-E) Typical photographs of colons and the variation of colon length from different treated groups. (F-G) Photographs of Spleen (F) and statistics of spleen index (weight ratio of spleen and the whole body) in colitis mice. (H-I) Representative H&E images and histological scores of colons from each group. Scale bar: 500 μm (top row), 200 μm (bottom row). (J) The expression of IL-6 in plasma determined by ELISA Kit. (K-M) The level of IL-6, IL-1β and TNF-α in colon tissue determined using Q-PCR. **p* < 0.05, ***p* < 0.01, ****p* < 0.001, *****p* < 0.0001, ns, no significant differences (*n* = 5)

Real-Time fluorescent quantitative PCR (RT-qPCR). The RNA from colon tissue samples was extracted using the Trizol isolation reagent according to the manufacturer's directions. Reverse transcription reaction was conducted using Transcriptor First Strand cDNA Synthesis Kit (Roche, Inc., Basel, Switzerland). Quantitative real-time PCR analysis was performed using real-time PCR ViiATM7 with SYBR Green master mix (Roche, Inc., Basel, Switzerland). The relative expressions of mRNA were calculated using the $2^{-\Delta\Delta C_t}$ comparative method. The primers were used as follows: TNF- α , forward primer: GTCAGGTTGCCCTCTGTCTCA, reverse primer: TCAGGGAAGAGTCTGGAAAG; IL-6, forward primer: TAGTCCTTCCACCCCAATTCC, reverse primer: TTGGTCCTTAGCCACTCCTTC; GAPDH, forward primer: AGGTCGGTGTGAACGGATTTG, reverse primer: TGTAGACCATGTAGTTGAGGTCA; IL-1 β , forward primer: GAAATGCCACCTTTTGACAGTG, reverse primer: TGGATGCTCTCATCAGGACAG.

Histology

The colon, spleen, liver, lung, kidney, and heart collected from mice with different treatments were fixed by 5 min instillation of 10% formalin through trachea catheterization at a trans-pulmonary pressure of 15 cm H₂O, and then fixed in 10% formalin at room temperature for 48 h. After that, tissues were embedded in paraffin, cut into 5 μ m sections, and stained with hematoxylin and eosin (H&E). For further detect the changes in NLRP3 antibodies in colons, the colon sections were also stained with NLRP3 antibodies.

TUNEL staining

Lung tissue sections were deparaffinized by placing them in an oven at 60 °C for 15 min and then treated with xylene for further dewaxing. After hydration with ethanol and distilled water, the tissue sections were permeabilized using proteinase K at 37 °C for 30 min. Subsequently, the sections were washed three times with PBS and incubated with 100 μ L of TUNEL staining solution at 37 °C for 1 h. Following another round of washing with PBS, the tissues were sealed with DAPI anti-fluorescence quencher.

ROS scavenging ability in RAW 264.7 cells

The cells were planted in 6-well culture plates for 12 h, then fresh standard growth medium containing different formulations of Nar was added and further incubated for 24 h. Next a fresh medium containing 1 μ g/mL LPS was used to induce ROS production for 6 h except the negative group. Then, the cells were incubated with DCFH-DA (Beyotime Biotechnology, China) for 30 min in dark at 37 °C, washed with PBS for three times, collected by centrifugation and analyzed by a Live Cell

Imaging System (EVOSFL Auto, Invitrogen, USA) or a flow cytometer at 488 nm of excitation wavelength and 525 nm of emission wavelength.

Determination of ROS level in colon tissues

For DHE staining of colon sections, 1 μ mol L⁻¹ Dihydroethidium (DHE) solution was dropped on the colon tissue sections, and incubated at 37 °C in the dark for 20 min. Next, the samples were washed with PBS for 3 \times 5 min. Before mounting, samples were incubated with 4',6-diamidino-2-phenylindole (DAPI) for 5 min at room temperature and washed three times with PBS for 5 min. All steps were performed in the dark on a shaker. Finally, the red fluorescence intensity was observed under a fluorescence microscope.

Statistical analysis

Results were expressed as mean \pm SD. Statistical significance was determined by one-way ANOVA with a Games-Howell post hoc analysis for multiple-group comparisons. Two-group comparisons were analyzed by the two-tailed unpaired Student t -test.

Results and discussion

Characteristic of MC@Nar-NPs

Currently, the treatment of IBD mainly relies on anti-inflammatory drugs and immunosuppressants, which can be administered via injection, oral ingestion, or rectal application. However, these treatment regimens are often associated with adverse reactions, and it is challenging to maintain effective drug concentrations locally [17]. Therefore, there is an urgent need for new drug targeting delivery systems, such as targeted nanoparticle drug delivery systems, to increase drug solubility, prolong drug residence time in the intestine, target drug delivery to the site of inflammation, enhance drug bioavailability, and reduce potential adverse reactions [18]. Here, mannose and chitosan modified PLGA-PEG nanoparticles to load Nar and deliver Nar (MC@Nar-NPs) to the colons. The SEM (scanning electron microscope) image revealed that the as-synthesized nanoparticles displayed a uniform spherical shape (Fig. 1A). The physico-chemical properties of the MC@Nar-NPs were investigated using Fourier transform infrared (FT-IR) spectroscopy. The results suggested that there were no significant shifts or losses of functional group peaks in the characteristic spectral peaks, indicating that there was no chemical interaction between the drug and the polymer during the nanocapsulation process. This is supported by the retention of the characteristic peaks of both the polymer and the drug in the FT-IR spectra of the MC@Nar-NPs (Fig. 1B). The UV-vis spectrum of the NPs was measured to assess the loading of Nar within the NPs (Fig. 1C). The absorption spectrum of Nar exhibited characteristic absorption

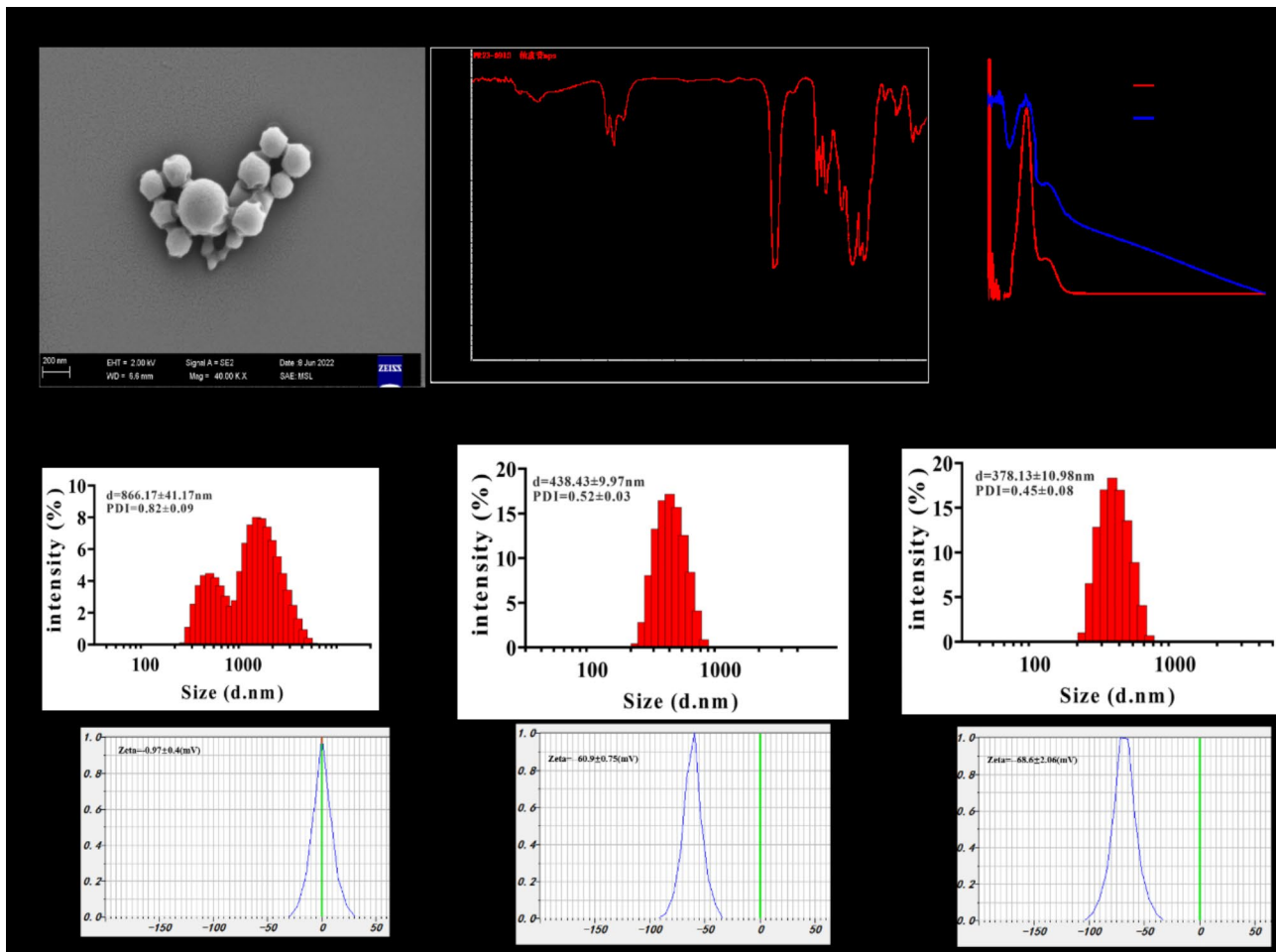


Fig. 1 Characteristic of MC@Nar-NPs. (A) Representative morphology image of MC@Nar-NPs determined by scanning electron microscope (1 bar = 200 nm). (B) FT-IR spectra of chitosan, mannose, PLGA-PEG, Nar and MC@Nar-NPs. (C) UV-vis spectra of free Nar and MC@Nar-NPs. (D-F) Size distribution and zeta potential of the as-synthesized MC@Nar-NPs in different pH solutions (pH = 2, 6 and 8), respectively

peaks at 283 nm. The absorption spectrum of the Nar-NPs closely resembled that of free Nar, indicating successful encapsulation of Nar within the NPs. The loading capacity of Nar in the MC@Nar-NPs was approximately 9.1%, which was calculated based on the standard curve of Nar at its UV absorption peak of 283 nm.

Oral administration is the most preferred route of administration with the highest patient compliance, while oral medications need to undergo degradation and dissolution in the gastrointestinal tract and gastric fluid [19]. In order to evaluate the ability of the prepared nanoparticles to resist gastric fluid corrosion (pH = 1 ~ 2) and achieve targeted accumulation at the site of colitis (pH = 7 ~ 8), we tested the size and zeta potential of the nanoparticles using dynamic light scattering (DLS) under different pH environments. It showed the sizes and zeta potential of MC@Nar-NPs were ~900 nm and ~+1 mV in pH = 2 solution which mimics gastric acid environment (Fig. 1D). And, the sizes and zeta potential of MC@Nar-NPs were ~400 nm and ~-60 mV in pH = 6 solution

which mimics small intestine environment (Fig. 1E). While, the sizes and zeta potential of MC@Nar-NPs were changed into ~400 nm and ~-68 mV in pH = 8 solution which mimics colon environment (Fig. 1F). These data demonstrate that MC@Nar-NPs tend to aggregate together and stay relatively stable in stomach, and tend to disperse in intestines. Interestingly, the massive negative charges on the surface of MC@Nar-NPs in pH = 8 render them to target and retain into the IBD lesion-specific positive charges [20].

Stability of MC@Nar-NPs under different pH solutions

For the oral delivery of MC@Nar-NPs being suitable for IBD therapy, it is critical to keep contact nanostructure or nano-assembly in the stomach and small intestine, especially in the strong acid condition of stomach, which is still a great challenge for most nano-delivery systems. To investigate the source of the negative charges of MC@Nar-NPs, we assayed the zeta potentials of the four kinds of nanoparticles, e.g. Nar-NPs, chitosan modified

Nar-NPs, mannose modified Nar-NPs and both chitosan and mannose modified Nar-NPs. The results indicated that all the four kinds of NPs were negative charged, while, the absolute value of MC@Nar-NPs is much more than that of CS@Nar-NPs and Man@Nar-NPs. So, we think that the negatively charges of NPs are resulted from the chitosan and mannose modification (shown in the supplemental results Figure S1).

To investigate the stability of MC@Nar-NPs in the digestive tract, we evaluated the characteristics of the NPs in different pH conditions for 8 days (Fig. 2A). The pH=2, pH=6 and pH=8 solution was simulated the environments of stomach, intestine and colon, respectively. In the pH=2 solution, the size (Fig. 2B) of MC@Nar-NPs kept aggregated for more than 1000 nm, and the size distribution decreased, but still larger than 800 nm

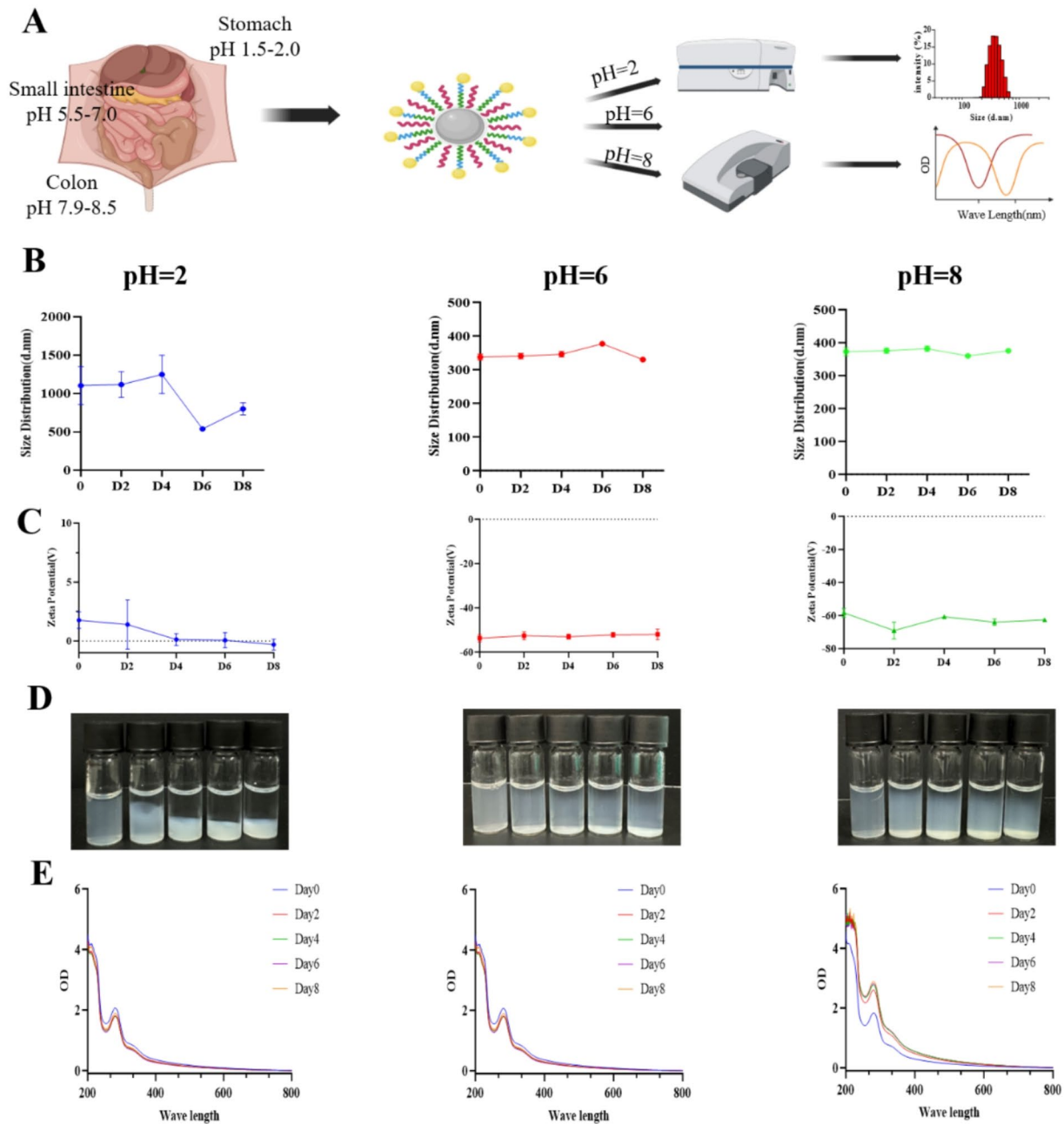


Fig. 2 The storage stability of MC@Nar-NPs. (A) The pH range of gastrointestinal tract. (B) Changes of particle size of MC@Nar-NPs in solutions of pH=2, 6, and 8. (C) Changes of zeta potential of MC@Nar-NPs in solutions of pH=2, 6, and 8. (D) The photos pf appearance color changes of MC@Nar-NPs at three different pH conditions during the storage. (E) Changes of absorbance of MC@Nar-NPs under different pH condition

after 8 days, and the picture of NPs solution showed the precipitate of NPs after 2 days. And, the zeta potential of NPs (Fig. 2C) was positive, indicating they were hard retained by stomach. Besides, the UV-vis spectra (Fig. 2E) showed the Nar almost did not release from the NPs during the first 8 days. This implied that this oral NPs system was stable and could successfully endure the strong acid condition of stomach. Interestingly, in pH=6 and pH=8 solution, the NPs dispersed evenly (Fig. 3B), displayed massive negative charges on the surface (Fig. 3C), and the

UV-vis also demonstrated the released Nar from MC@Nar-NPs (Fig. 3E). Further, to detect the in vitro release kinetics of Nar, we used centrifugation method according to the previous reports [21] with a little modification. In brief, take 10 mL of pH 7.4 PBS buffer as the release medium, dissolve the nanomedicine equivalent to 1 mg of Nar into PBS, and then, keep constantly shaking at the speed of 120 rpm at 37 °C in dark. 3 mL of sample was taken out and 3 mL of PBS was simultaneously added at designated time points (0.5 h, 1 h, 1.5 h, 2 h, 4 h, 6 h, 12 h,

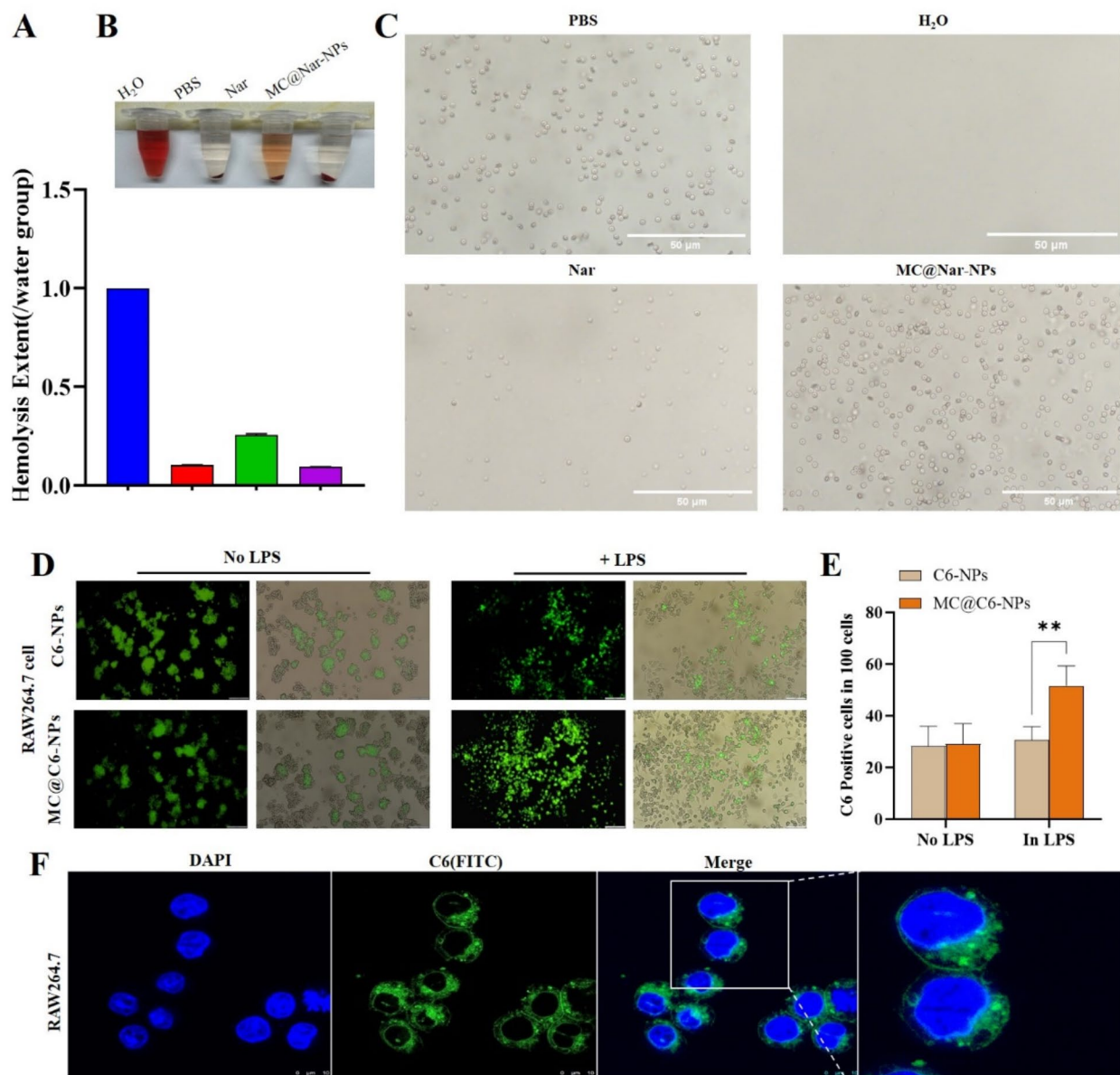


Fig. 3 In vitro biosafety and biocompatibility of Nar and MC@Nar-NPs. (A, B) The photos and quantification analysis of hemolysis assay of free Nar and MC@Nar-NPs. (C) The morphology of erythrocytes co-cultured with Nar or MC@Nar-NPs for 30 min at 37 °C imaged under a live cell imaging system. Scale bars: 50 μm. (D-F) Cell uptake of differently modified nanoparticle-based systems. Due to the weak fluorescence of Nar, Coumarin 6 (C6) was co-loaded into the NPs as fluorescent markers. (D-E) Cell uptake of C6/Nar-NPs or MC@C6/Nar-NPs by RAW264.7 cells with or without LPS induction. Scale bars: 100 μm. (F) Confocal images of MC@C6/Nar-NPs in RAW264.7 cells. Scale bars: 10 μm

24 h, 36 h, 48 h, 60 h, 84 h). The isolated samples were centrifuged at 10000 rpm, 25 °C for 10 min, and the concentration of Nar in the supernatant were assayed to calculate the cumulative drug release. The experiment was carried out three times in parallel, and the results were averaged. The results (supplemental results Figure S3) showed that around 40% of Nar were released during the first 2 h, and about 50% of Nar were released from 2 h to 84 h, implying that the NPs formulation had a sustained release effect.

In vitro biosafety and biocompatibility of MC@Nar-NPs

The hemolytic potential of a drug is a crucial metric for determining whether it can induce hemolysis, which is the destruction of red blood cells upon administration into the body [22]. In this study, the hemolytic effects of Nar (a drug name, presumably) and MC@Nar-NPs (presumably a nanoparticle formulation of Nar) were assessed using healthy mouse erythrocytes. Erythrocytes suspended in water served as the positive control for hemolysis, while those in PBS (phosphate-buffered saline) buffer constituted the normal control group. Both free Nar and MC@Nar-NPs were introduced to the erythrocytes at an equivalent concentration of 10 mg/mL, based on the amount of Nar encapsulated within the nanoparticles. Figure 3A-C illustrate that free Nar caused significant damage to erythrocytes and exhibited hemolytic activity. In contrast, as anticipated, MC@Nar-NPs displayed minimal damage, preserving the healthy, intact double concave disc shape of the erythrocytes. This finding suggests that the nanoparticle formulation significantly mitigated hemolysis and enhanced the biosafety profile of Nar.

Intestinal macrophages are one of the main regulatory cells that maintain tissue microenvironmental homeostasis and a normal immune barrier [23]. They help the host fight against pathogens and microbes, reduce inflammation, and promote the repair of intestinal mucosal damage by regulating apoptosis and growth factor levels. Therefore, the development of efficient macrophage-targeted nanoparticles is of great significance for the precise treatment of inflammatory bowel diseases.

To ascertain the *in vitro* targeting efficacy of MC@Nar-NPs, the RAW264.7 cell line was utilized as a cellular model. Following a 2-hour co-culture period, the nanoparticles were observed to have successfully internalized into the cells, as evidenced by fluorescent imaging (Fig. 3D-E). Notably, the fluorescence intensity within the cells (Fig. 3E) suggested that the cellular uptake of MC@Nar-NPs was significantly higher in lipopolysaccharide (LPS)-stimulated RAW264.7 cells compared to that in resting RAW264.7 cells. This differential uptake may be attributed to the interaction with the mannose receptor, which is upregulated on LPS-stimulated RAW264.7

cells. Additionally, confocal microscopy images (Fig. 3F) revealed that the MC@Nar-NPs were uniformly dispersed throughout the cytoplasm, with no detectable penetration into the nucleus.

In vivo targeting of MC@Nar-NPs

One of the biggest challenges to treating IBD is to target the site of inflammation [6]. To determine the targeting ability of MC@Nar-NPs, indocyanine green (ICG) was encapsulated within nanoparticles (NPs), specifically MC@ICG/Nar-NPs, and utilized as a fluorescent marker. Both the free ICG/Nar formulation and the MC@ICG/Nar-NPs were orally administered to two groups: healthy mice (Fig. 4A-G) and mice with ulcerative colitis (UC) (Fig. 4H-N). Using an *in vivo* imaging system (IVIS), we observed the distribution post-administration. In healthy mice, the mean fluorescence intensity (MFI) upon oral administration of either free ICG/Nar or MC@ICG/Nar-NPs showed no significant differences (Fig. 4A-G). Notably, gastrointestinal (GI) tract imaging revealed that neither ICG/Nar nor MC@ICG/Nar-NPs accumulated or were retained in the healthy colons at 8–24 h post-administration. In contrast, in UC mice, the MFI in the MC@ICG/Nar-NPs group was substantially higher than that in the free ICG/Nar group at 8 and 24 h after oral administration. GI tract imaging particularly demonstrated that MC@ICG/Nar-NPs predominantly accumulated in the inflamed colonic regions at both 8 and 24 h, with a prolonged retention and release profile in the colons (Fig. 4H-N). At the 24-hour mark post-administration, only a minimal presence of MC@ICG/Nar-NPs was detected in the liver, with no significant accumulation observed in other organs, indicating that MC@Nar-NPs may not accumulate extensively in major organs of UC mice. These findings further corroborate that MC@ICG/Nar-NPs exhibit a preferential targeting to inflammatory lesions, a characteristic that was also supported by the *in vitro* cellular uptake assays.

Therapeutic efficacy of MC@Nar-NPs against DSS-Induced colitis

We subsequently evaluated the *in vivo* therapeutic efficacy of MC@Nar-NPs in a mouse model of DSS-induced UC. Mice were orally administered with 2.5% DSS for 5 days to induce colitis, and MC@Nar-NPs were daily oral administered of different compounds (Fig. 5A). Other treatments, including saline, free Nar, were used as control groups. From day 4 to day 7, bloody stools emerged in the DSS+ and DSS+Nar groups and bloody diarrhea was more severe in these groups. Only the mice in the MC@Nar-NPs treatment group had less stool blood. As shown in Fig. 5B, the PBS-treated control group failed to prevent body weight loss, whereas DSS-colitis mice with MC@Nar-NPs treatment could significantly recover their

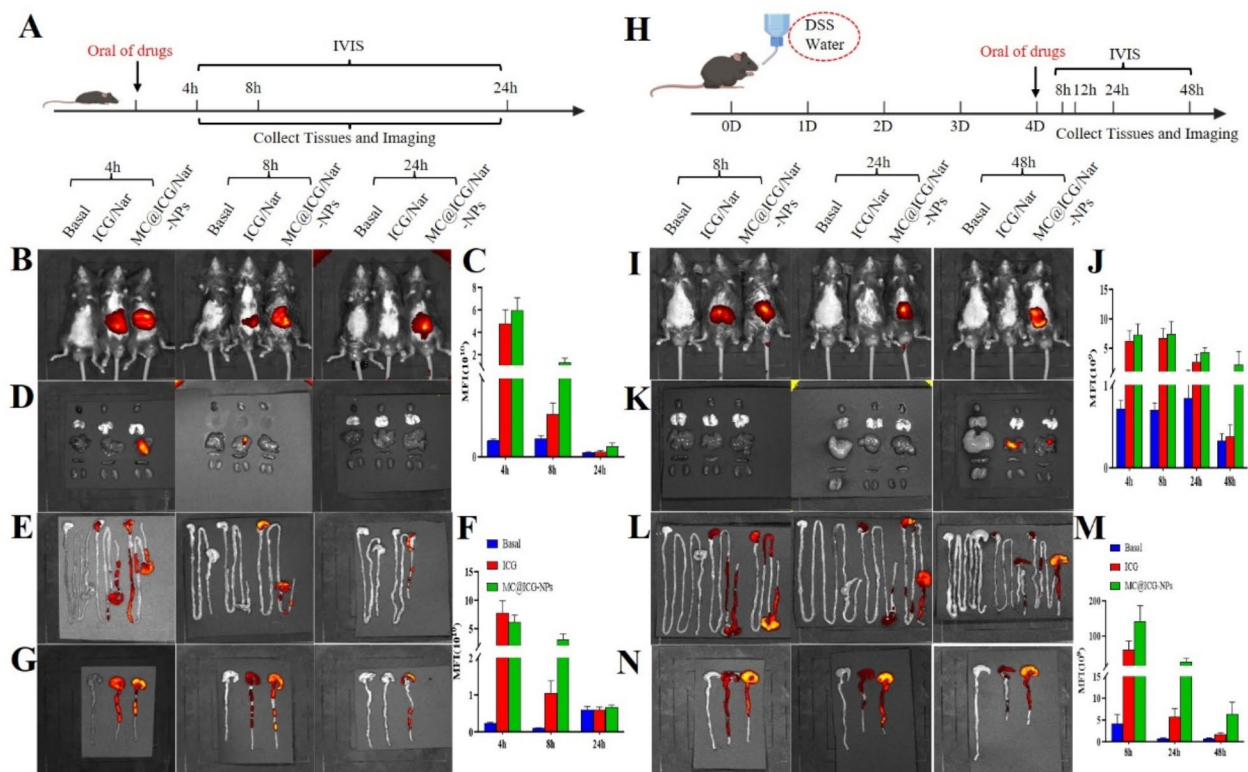


Fig. 4 In vivo targeting of MC@Nar-NPs. Due to the weak fluorescence of Nar, indocyanine green (ICG) was co-loaded into the NPs as fluorescent markers. **(A–G)** In vivo imaging of healthy mice with intra-gavage (i.g.) administration of Free-ICG/Nar or MC@ICG/Nar-NPs at different time points: **(A)** experimental protocols of IVIS imaging of Free-ICG/Nar or MC@ICG/Nar-NPs in healthy mice, i.g. healthy mice were oral administrated with Free-ICG/Nar or MC@ICG/Nar-NPs, after 4 h, 8 h, and 24 h, the whole body, main organs, and gastrointestinal tract were originated for IVIS imaging. **(I–J)** The images and MFI (mean fluorescence intensity) of ICG in the whole body of healthy mice. **(K)** The main organs originated from the above mice. **(E–F)** The images and MFI (mean fluorescence intensity) of ICG in the gastrointestinal tract of healthy mice. **(G)** The images of ICG in the colons of healthy mice. **(H–N)** In vivo imaging of UC mice with intra-gavage (i.g.) administration of Free-ICG/Nar or MC@ICG/Nar-NPs at different time points: **(H)** experimental protocols of IVIS imaging of Free-ICG/Nar or MC@ICG/Nar-NPs in UC mice, i.g. healthy mice drink DSS water (2.5%, w/v) for 4 days to induce colitis, and then were oral administrated with Free-ICG/Nar or MC@ICG/Nar-NPs, after 4 h, 8 h, 24 h and 48 h, the whole body, main organs, and gastrointestinal tract were originated for IVIS imaging. **(B–C)** The images and MFI (mean fluorescence intensity) of ICG in the whole body of UC mice. **(D)** The main organs originated from the above mice. **(L–M)** The images and MFI (mean fluorescence intensity) of ICG in the gastrointestinal tract of UC mice. **(N)** The images of ICG in the colons of UC mice. Data are expressed as mean \pm SD ($n=4$). * $p < 0.05$, ** $p < 0.01$, and *** $p < 0.001$

bodyweight. Inflammation severity, including weight loss, stool consistency and bloody stool, was further assessed by the disease activity index (DAI) score [24]. The results indicated that the DAI score of MC@Nar-NPs treatment was significantly lower than that in PBS-treated colitis mice (Fig. 5C). Furthermore, the gross colon appearance and colon length measurement showed that colon length was significantly shortened in colitis mice, while MC@Nar-NPs significantly protected mice against DSS-induced shortening of colon length (Fig. 5D, E). DSS also stimulated spleen enlargement and MC@Nar-NPs treatment could alleviate this phenomenon (Fig. 5F, G). H&E staining images (Fig. 5H) of colon tissues demonstrated obvious colonic damage and inflammatory infiltration in colitis mice. The mucin content on the inflamed colonic mucosa was very low, which was associated with mass depletion of goblet cells. Notably, the colonic tissue

morphology in MC@Nar-NPs treated group was almost similar to that of healthy mice. The histological scores (Fig. 5I) also showed that the oral MC@Nar-NPs treatment was beneficial for restoring the integrity of the colonic epithelium and alleviating the inflammatory cells infiltration at the mucosa, suggesting normal recovery of the colon tissue. To further understand the therapeutic mechanism of MC@Nar-NPs against colitis, the levels of several pro-inflammatory cytokines in plasma and colon tissues were quantified. As shown in Fig. 5J–M, among all groups, MC@Nar-NPs treatment significantly reduced the levels of pro-inflammatory cytokine IL-6 in plasma and the level of IL-6, IL-1 β and TNF- α in colons, indicating that the MC@Nar-NPs could effectively inhibit the inflammation responses in colitis mice.

Immunohistochemistry staining of colon tissues

The overproduction of reactive ROS is a crucial factor in the pathogenesis of inflammatory bowel disease (IBD), and the elimination of ROS in the inflamed colon has been established as an effective therapeutic approach [25]. Our study utilized DHE staining to assess the *in vivo* ROS-scavenging capacity of MC@Nar-NPs in colonic tissues. The DHE fluorescence, which appears red in the healthy control group, was notably weaker compared to the DSS-induced group, indicating a significant increase in ROS production due to DSS. Treatment with Nar, particularly in the form of MC@Nar-NPs, substantially reduced ROS levels in the colonic tissues (Fig. 6A-B). The *in vitro* ROS assay also showed LPS could induce the

overproduction of ROS in RAW264.7 cells, while with Nar, especially with MC@Nar-NPs, the ROS level was significantly reduced (supplemental results Figure S5), which was consistent with the *in vivo* data.

These findings underscore the potent ROS-scavenging properties of MC@Nar-NPs, contrasting with the free Nar at an equivalent dose, which failed to effectively suppress ROS production in DSS-treated mice. The NLRP3 inflammasome is recognized as a key modulator of mucosal immune responses and intestinal homeostasis [26]. Targeting the activation of the NLRP3 inflammasome and its downstream signaling pathways offers a promising avenue for developing novel therapeutic strategies for IBD. Consistent with our hypothesis, treatment

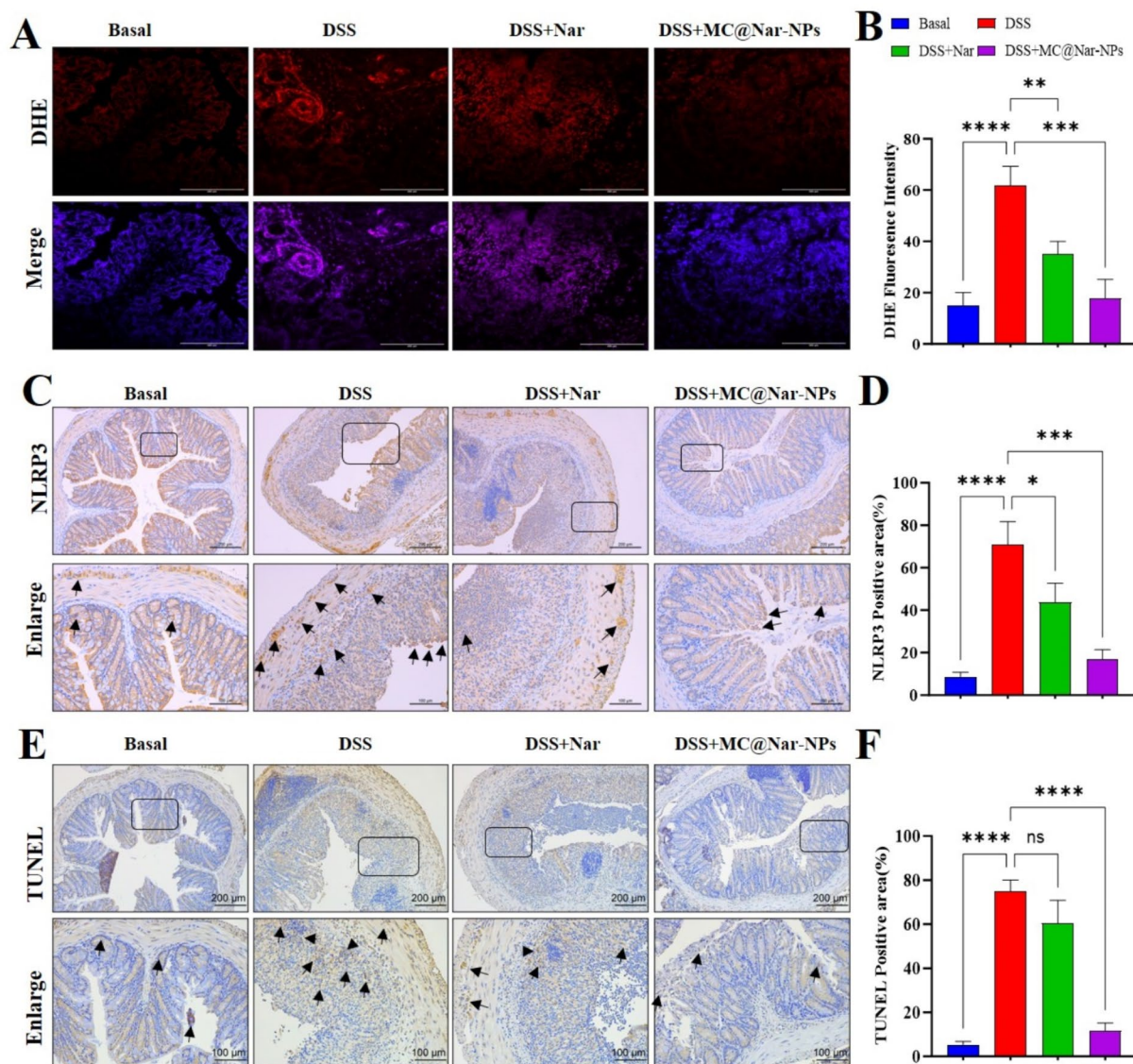


Fig. 6 Immunohistochemical staining of ROS, NLRP3 inflammasomes and apoptosis in colon sections. The representative images and their semi-quantitative analysis of ROS level (A-B), NLRP3 (C-D) and TUNEL (E-F) in the colon section of colitis mice. Mean \pm SEM, * $p < 0.05$, ** $p < 0.01$, *** $p < 0.001$, **** $p < 0.0001$, ns, no significant differences ($n = 5$)

with MC@Nar-NPs significantly dampened the activation of the NLRP3 inflammasome, suggesting that MC@Nar-NPs are effective in mitigating colonic inflammation (Fig. 6C-D). Epithelial cell apoptosis is known to be elevated in UC, and this increased rate of apoptosis can expose the mucosa to luminal pathogens, potentially contributing to the disease's pathogenesis. As referenced in the literature [27], Fig. 6E-F illustrate that both Nar and MC@Nar-NPs treatments led to a significant reduction in the apoptosis rate of epithelial cells in the inflamed colon. Collectively, these results suggest that the therapeutic benefits of Nar, particularly when delivered via MC@Nar-NPs, in a DSS-induced UC model may be attributed to the combined effects of ROS elimination, NLRP3 inflammasome inactivation, and a reduction in epithelial apoptosis.

In vivo biosafety

In order to assess the in vivo toxicity of Nar or MC@Nar-NPs, we harvested the principal organs—excluding the lungs—from mice with ulcerative colitis (UC) that had undergone various treatments. Subsequently, these

organs were subjected to hematoxylin and eosin (H&E) staining. The findings, as depicted in Fig. 7A, indicated no significant morphological differences across the organs of mice in all experimental groups. Additionally, liver function was evaluated through measurements of alanine transaminase (ALT) and aspartate transaminase (AST), with results shown in Fig. 7B and C, respectively. No notable alterations were observed in these liver enzymes. Collectively, these observations underscore the biosafety profile of MC@Nar-NPs in the context of UC treatment.

Impact of MC@Nar-NPs on gut microbiota

The gut microbiota is a critical factor affecting the intestines [28]. Therefore, we used 16s rRNA sequencing to analyze the microbiota carried in the feces of mice to determine whether NPs treat dss-induced colitis by altering the gut microbiota. Figure 8A shows that the Venn diagram indicates a total of 223 shared species among the samples. The dilution curve directly reflects the rationality of the sequencing data quantity; the curve in Fig. 8B tends to flatten, indicating that the sequencing

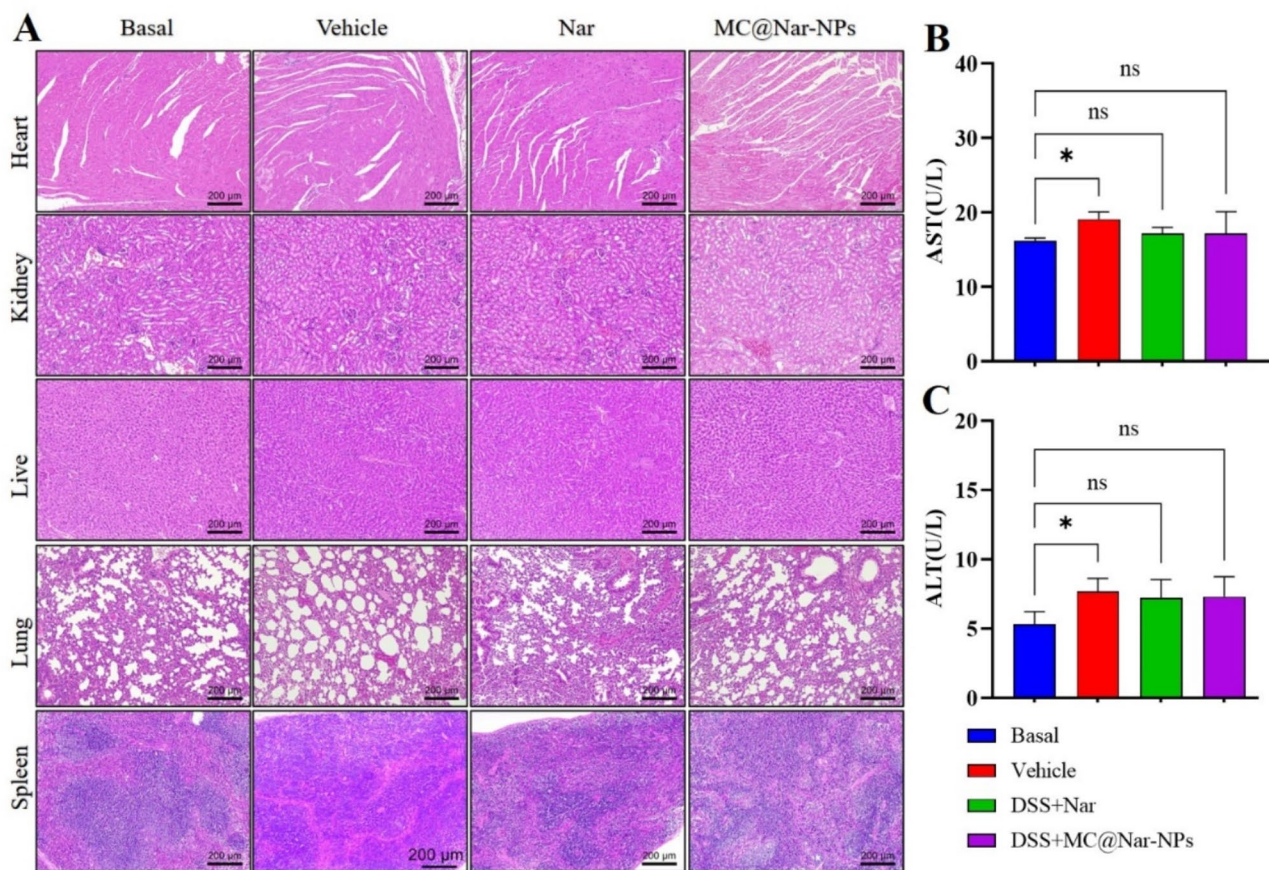


Fig. 7 The in vivo biosafety of different formulations of Nar. (A) Typical photos of main organs originated from UC mice with oral administration of different compounds for 7 days (once a day) at 10 mg/kg body weight. 1 bar = 200 µm. (B-C) The levels of aspartate transaminase (AST) and alanine transaminase (ALT) of livers in each group were tested to evaluate the toxicity of different formulations of Nar

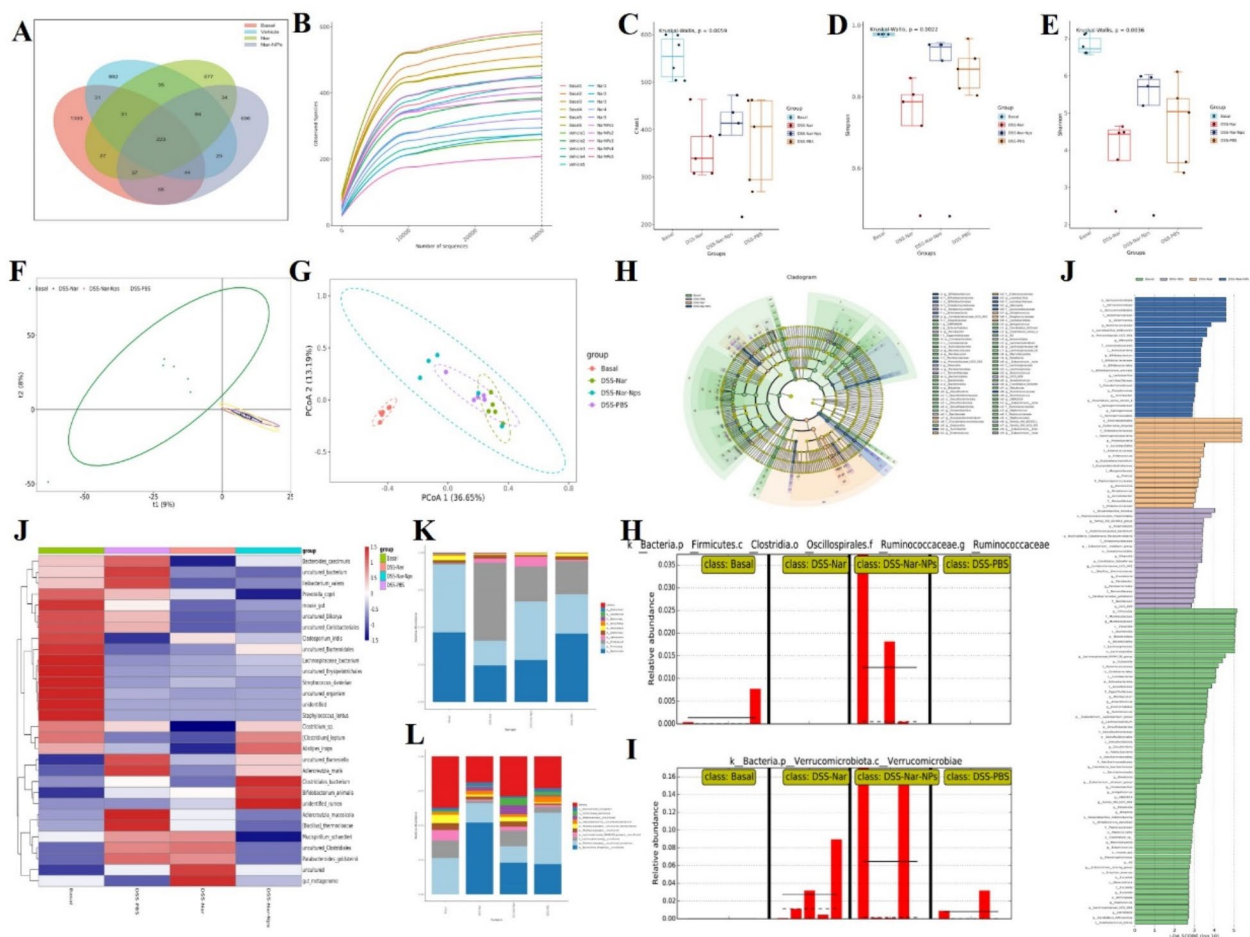


Fig. 8 Diversity and composition analysis of gut microbiota in different treated groups: (A) Venn diagram showed common species comparison with the four groups. (B) Rarefaction curves (C-E) α -diversity indices. (F) PCA analysis. (G) PCoA analysis. **The relative abundance of gut flora in mice with DSS-induced UC:** (J) The heatmap analysis. (K) The relative abundance of gut flora categorized by Phylum. (L) The relative abundance of gut flora categorized by Genus. **The results of LEfSe analysis:** (H) The Cladogram results. (H-I) The relative abundance of Ruminococcaceae and Verrucomicrobiae as Biomaker in each group. (J) The LDA score (log 10) of each group

data quantity is reasonable and the sequencing results are credible. The Chao1 index, Simpson index, and Shannon index were all significantly reduced ($p < 0.05$ or $p < 0.01$), indicating a decrease in community abundance and diversity (Fig. 8C-E). β -diversity analysis was used to assess the differences in microbial community structures, and the results showed that the intestinal microbiota of the mice significantly changed after DSS treatment, and the medication group improved their intestinal microbiota (Fig. 8F-G). According to the species annotation results, select the top 10 species in terms of maximum abundance at the phylum and species classification levels in each group, and generate a cumulative bar chart of the relative abundance of species. As shown in Fig. 8I-K, at the phylum level, the relative abundance of Bacteroidetes in the DSS group remains almost unchanged, while the relative abundance of Firmicutes decreases and the relative abundance of Proteobacteria increases; after

treatment with nanomedicine, the relative abundance of Bacteroidetes decreases and the relative abundance of Firmicutes increases. At the genus level, the most affected is Lachnospiraceae. Furthermore, according to the results of heatmap analysis, the nanomedicine group improved the imbalance of intestinal flora, increased the relative abundance of Bifidobacterium, Clostridiales, and Alistipes, and decreased the relative abundance of Adlercreutzia, Bacillus, and Parabacteroides. LEfSe analysis performs linear discriminant analysis (LDA) on samples based on taxonomic composition to identify communities or species that significantly affect the classification of samples. The results show that a total of 125 taxonomic groups were obtained from phylum to genus, including 63 in the Basal group, 20 in the DSS group, 18 in the parent drug group, and 24 in the nanomedicine group (Fig. 8H, L-N). In the Basal group, Firmicutes, Muribaculaceae, Clostridia, and Bacteroidia are the main flora;

the dominant flora in the DSS group are *Oceanobacillus*, *Peptostreptococcales*, and *Anaerostipes*; *Enterobacteriaceae*, *Gammaproteobacteria*, and *Proteobacteria* play a major role in the parent drug group; and the dominant flora in the nanomedicine group are *Verrucomicrobiota* and *Ruminococcaceae*, with their relative abundance significantly higher than the other three groups, indicating that nanomedicines can produce therapeutic effects by regulating the intestinal microbiota.

Conclusion

In this study, we have successfully designed novel orally bioavailable colon-targeted nanoparticles for the precise delivery of Nar to alleviate ulcerative colitis (UC) in mice. The MC@Nar-NPs exhibited exceptional properties, including a high encapsulation efficiency and strong colon-targeting capability. The MC@Nar-NPs not only effectively mitigated the symptoms of DSS-induced colitis by repairing intestinal injury but also demonstrated abilities to downregulate oxidative stress and reduce the expression levels of inflammatory cytokines, while modulating inflammation-related signaling pathways. Additionally, the nanoparticles were found to restore the composition of the gut microbiota. Overall, our findings suggest a promising future for MC@Nar-NPs as an oral nutrient delivery system for the treatment of UC.

Supplementary Information

The online version contains supplementary material available at <https://doi.org/10.1186/s12967-024-05662-1>.

Supplementary Material 1

Acknowledgements

This work was supported by the Natural Science Foundation of Guangdong Province (2022A1515140154), the Science Foundation of Dongguan Science and Technology Bureau (20211800905092), the Scientific research project of general universities in Guangdong province (2021KTSCX033), Guangdong Medical University post doctor Fund (1026/4SG23180G), Guangdong Provincial Medical Research Fund (A2024676). Construction Project of Nano Technology and Application Engineering Research Center of Guangdong Medical University (45G24179G).

Author contributions

Hua Jin and Zhikun Zhou led the study; Shilong Fan, Yue Zhao and Yinlian Yao contributed equally to this work. Shilong Fan, Yue Zhao and Yinlian Yao conceived the study; Xin Shen, Xingxing Chai and Jiahui Li participated in the animal experiments; Jiang Pi and Xueqin Huang were responsible for the data analysis; Hua Jin wrote the manuscript; Hua Jin and Zhikun Zhou Provide funding and general guidance.

Declarations

Ethics approval and consent to participate

Experimental procedures using mice in this study were reviewed and approved by the ethical review board of Guangdong Medical University, and all the experiments were performed in accordance with relevant guidelines and regulations of Animal Ethics Committee of Guangdong Province, China. Animals and protocol were approved by the Ethics Committee of Guangdong Medical University (GDY2002004).

Conflicts of interest

The authors declare that they have no conflicts of interest.

Competing interests

The authors declare that they have no competing interests.

Received: 22 May 2024 / Accepted: 9 September 2024

Published online: 30 September 2024

References

1. Gajendran M, Loganathan P, Jimenez G, Catinella AP, Ng N, Umapathy C, Ziade N, Hashash JG. A comprehensive review and update on ulcerative colitis(). *Dis Mon.* 2019;65:100851.
2. Ordás I, Eckmann L, Talamini M, Baumgart DC, Sandborn WJ. Ulcerative colitis. *Lancet.* 2012;380:1606–19.
3. Perrotta C, Pellegrino P, Moroni E, De Palma C, Cervia D, Danelli P, Clementi E. Five-aminosalicylic Acid: an update for the reappraisal of an old drug. *Gastroenterol Res Pract* 2015, 2015:456895.
4. Bruscoli S, Febo M, Riccardi C, Migliorati G. Glucocorticoid therapy in inflammatory bowel disease: mechanisms and clinical practice. *Front Immunol.* 2021;12:691480.
5. Kayal M, Shah S. Ulcerative Colitis: current and emerging treatment strategies. *J Clin Med* 2019, 9.
6. Zhang M, Merlin D. Nanoparticle-based oral drug Delivery systems Targeting the Colon for treatment of Ulcerative Colitis. *Inflamm Bowel Dis.* 2018;24:1401–15.
7. Liu L, Wu Y, Wang B, Jiang Y, Lin L, Li X, Yang S. DA-DRD5 signaling controls colitis by regulating colonic M1/M2 macrophage polarization. *Cell Death Dis.* 2021;12:500.
8. Long J, Liu XK, Kang ZP, Wang MX, Zhao HM, Huang JQ, Xiao QP, Liu DY, Zhong YB. Ginsenoside Rg1 ameliorated experimental colitis by regulating the balance of M1/M2 macrophage polarization and the homeostasis of intestinal flora. *Eur J Pharmacol.* 2022;917:174742.
9. Li ZL, Yang BC, Gao M, Xiao XF, Zhao SP, Liu ZL. Naringin improves sepsis-induced intestinal injury by modulating macrophage polarization via PPAR γ /miR-21 axis. *Mol Ther Nucleic Acids.* 2021;25:502–14.
10. Ma K, Liu W, Liu Q, Hu P, Bai L, Yu M, Yang Y. Naringenin facilitates M2 macrophage polarization after myocardial ischemia-reperfusion by promoting nuclear translocation of transcription factor EB and inhibiting the NLRP3 inflammasome pathway. *Environ Toxicol.* 2023;38:1405–19.
11. Shi J, Li J, Xu Z, Chen L, Luo R, Zhang C, Gao F, Zhang J, Fu C. Celastrol: a review of useful strategies overcoming its limitation in Anticancer Application. *Front Pharmacol.* 2020;11:558741.
12. Cao H, Liu J, Shen P, Cai J, Han Y, Zhu K, Fu Y, Zhang N, Zhang Z, Cao Y. Protective effect of Naringin on DSS-Induced Ulcerative Colitis in mice. *J Agric Food Chem.* 2018;66:13133–40.
13. Zu M, Ma Y, Cannup B, Xie D, Jung Y, Zhang J, Yang C, Gao F, Merlin D, Xiao B. Oral delivery of natural active small molecules by polymeric nanoparticles for the treatment of inflammatory bowel diseases. *Adv Drug Deliv Rev.* 2021;176:113887.
14. Jin H, Pi J, Zhao Y, Jiang J, Li T, Zeng X, Yang P, Evans CE, Cai J. EGFR-targeting PLGA-PEG nanoparticles as a curcumin delivery system for breast cancer therapy. *Nanoscale.* 2017;9:16365–74.
15. Jin H, Luo R, Li J, Zhao H, Ouyang S, Yao Y, Chen D, Ling Z, Zhu W, Chen M, et al. Inhaled platelet vesicle-decoyed biomimetic nanoparticles attenuate inflammatory lung injury. *Front Pharmacol.* 2022;13:1050224.
16. Hidalgo-Cantabrana C, Algieri F, Rodriguez-Nogales A, Vezza T, Martínez-Cambor P, Margolles A, Ruas-Madiedo P, Gálvez J. Effect of a Ropy Exopolysaccharide-Producing *Bifidobacterium animalis* subsp. *lactis* strain orally administered on DSS-Induced Colitis mice Model. *Front Microbiol* 2016, 7.
17. Li X, Lu C, Yang Y, Yu C, Rao Y. Site-specific targeted drug delivery systems for the treatment of inflammatory bowel disease. *Biomed Pharmacother.* 2020;129:110486.
18. Lu L, Chen G, Qiu Y, Li M, Liu D, Hu D, Gu X, Xiao Z. Nanoparticle-based oral delivery systems for colon targeting: principles and design strategies. *Sci Bull.* 2016;61:670–81.
19. Li DF, Yang MF, Xu HM, Zhu MZ, Zhang Y, Tian CM, Nie YQ, Wang JY, Liang YJ, Yao J, Wang LS. Nanoparticles for oral delivery: targeted therapy for inflammatory bowel disease. *J Mater Chem B.* 2022;10:5853–72.

20. Song X, Huang Q, Yang Y, Ma L, Liu W, Ou C, Chen Q, Zhao T, Xiao Z, Wang M, et al. Efficient therapy of inflammatory bowel disease (IBD) with highly specific and durable targeted Ta(2) C modified with chondroitin sulfate (TACS). *Adv Mater*. 2023;35:e2301585.
21. Zhang H-Y, Sun C-y, Adu-Frimpong M, Yu J-n, Xu X-m: glutathione-sensitive PEGylated curcumin prodrug nanomicelles: Preparation, characterization, cellular uptake and bioavailability evaluation. *Int J Pharm*. 2019;555:270–9.
22. Choi J, Reipa V, Hitchins VM, Goering PL, Malinauskas RA. Physicochemical characterization and in vitro hemolysis evaluation of silver nanoparticles. *Toxicol Sci*. 2011;123:133–43.
23. Na YR, Stakenborg M, Seok SH, Matteoli G. Macrophages in intestinal inflammation and resolution: a potential therapeutic target in IBD. *Nat Rev Gastroenterol Hepatol*. 2019;16:531–43.
24. Kim JJ, Shajib MS, Manocha MM, Khan WI. Investigating intestinal inflammation in DSS-induced model of IBD. *J Vis Exp* 2012.
25. Bourgonje AR, Feelisch M, Faber KN, Pasch A, Dijkstra G, van Goor H. Oxidative stress and redox-modulating therapeutics in inflammatory bowel disease. *Trends Mol Med*. 2020;26:1034–46.
26. Song Y, Zhao Y, Ma Y, Wang Z, Rong L, Wang B, Zhang N. Biological functions of NLRP3 inflammasome: a therapeutic target in inflammatory bowel disease. *Cytokine Growth Factor Rev*. 2021;60:61–75.
27. Seidelin JB, Nielsen OH. Epithelial apoptosis: cause or consequence of ulcerative colitis? *Scand J Gastroenterol*. 2009;44:1429–34.
28. Hou K, Wu ZX, Chen XY, Wang JQ, Zhang D, Xiao C, Zhu D, Koya JB, Wei L, Li J, Chen ZS. Microbiota in health and diseases. *Signal Transduct Target Ther*. 2022;7:135.

Publisher's note

Springer Nature remains neutral with regard to jurisdictional claims in published maps and institutional affiliations.